Programmed Fabrication of Bimetallic Nanobarcodes for Miniature Multiplexing Bioanalysis

ARTICLE *in* ANALYTICAL CHEMISTRY · MARCH 2009

Impact Factor: 5.64 · DOI: 10.1021/ac802670q · Source: PubMed

5 AUTHORS, INCLUDING:

Wei-Ming Zhang
Wenzhou University
13 PUBLICATIONS **1,060** CITATIONS
SEE PROFILE

Jin-Song Hu
Chinese Academy of Sciences
76 PUBLICATIONS **6,937** CITATIONS
SEE PROFILE

Wei-Guo Song
Chinese Academy of Sciences
110 PUBLICATIONS **4,625** CITATIONS
SEE PROFILE

Anal. Chem. **2009,** *81,* 2815–2818

Programmed Fabrication of Bimetallic Nanobarcodes for Miniature Multiplexing Bioanalysis

Wei-Ming Zhang, Jin-Song Hu, Hai-Tao Ding, Li-Jun Wan,* and Wei-Guo Song*

Laboratory of Molecular Nanostructures and Nanotechnology, Institute of Chemistry, Chinese Academy of Sciences, Beijing 100190, P. R. China, and Beijing National Laboratory for Molecular Sciences (BNLMS), Beijing 100190, P. R. China

Nanobarcodes with Morse code patterns are fabricated by a programmed electrochemical deposition process. These bimetallic nanobarcodes are stable and easy to decode using optical or electrical devices. Their discretionally patterned codes offer mass memory capacity for information carriers. They show promising features as probe molecules' carriers in multiplexing bioanalysis.

Multiplexing bioanalysis using suspension arrays is a powerful method for analyzing biomolecules. A critical factor in suspension array is the usage of carriers to carry the probe molecules; and the carriers must contain certain identifiable codes to let researchers identify the probe molecule attached to it.[1−4] In the past few years, many methods were developed to prepare encoded particles as probe molecule carriers,[4,5] and the graphical encoding has become one of the most successful methods among these strategies.[6−16] "Smart Bead" has been developed to produce cell identification by the standard semiconductor microfabrication technique.[16] Though millions of different code combinations are possible in this design, each batch requires a predetermined mask that is produced by complicated lithography. Photobleaching various patterns onto fluorescent polymer microspheres[9] and microbarcodes using fused glass blocks doped with rare-earth ions[10] were also reported, but these encoding processes are very slow; thus their practical applications are limited. Multifunctional dot-encoded particles are prepared by continuous-flow lithography for multiplexing bioanalysis.[14] However, for accurate lithographic encoding and readout, these particles have to be about several hundreds micrometers in diameter, which may not be suitable for high-density bioanalysis.

Recently, submicrometer metallic barcode were fabricated by sequential electrochemical depositions.[6,8,11,12,17] These barcode rods can be identified by the reflectivity difference of different metals using optical microscopes and pattern-recognition software, but the number of the distinguishable codes is only about 500, which limits the scope of an array. Furthermore, the sequential electrochemical deposition method requires frequent switching of the electrobath solution, which is not only tedious but also leads to poor reproduction.

Nanobarcodes are ideal carriers for probe molecules if the number of codes is unlimited and the fabrication is facile. Recent progress of nanoscale pulse electrodeposition provides us a reliable route to produce multicomponent nanorods,[18−23] which can be used for the nanobarcode fabrication. In this study, we designed a programmed method to fabricate bimetallic nanobarcodes, including Co−Pt, NiCo−Pt, and Fe−Au nanobarcodes, with no bath switching. The nanobarcodes can be read by optical microscope combined with pattern recognition software. The

* Corresponding author. Fax: (+86) 10-62558934. E-mail: wanlijun@iccas.ac.cn (L.-J.W.); wsong@iccas.ac.cn (W.-G.S.).

(1) Fodor, S. P. A.; Rava, R. P.; Huang, X. C.; Pease, A. C.; Holmes, C. P.; Adams, C. L. *Nature* **1993**, *364* (6437), 555–556.
(2) MacBeath, G.; Schreiber, S. L. *Science* **2000**, *289* (5485), 1760–1763.
(3) Gershon, D. *Nature* **2002**, *416* (6883), 885–891.
(4) Wilson, R.; Cossins, A. R.; Spiller, D. G. *Angew. Chem., Int. Ed.* **2006**, *45* (37), 6104–6117.
(5) Finkel, N. H.; Lou, X. H.; Wang, C. Y.; He, L. *Anal. Chem.* **2004**, *76* (19), 353A–359A.
(6) Nicewarner-Pena, S. R.; Freeman, R. G.; Reiss, B. D.; He, L.; Pena, D. J.; Walton, I. D.; Cromer, R.; Keating, C. D.; Natan, M. J. *Science* **2001**, *294* (5540), 137–141.
(7) Matthias, S.; Schilling, J.; Nielsch, K.; Muller, F.; Wehrspohn, R. B.; Gosele, U. *Adv. Mater.* **2002**, *14* (22), 1618–1621.
(8) Walton, I. D.; Norton, S. M.; Balasingham, A.; He, L.; Oviso, D. F.; Gupta, D.; Raju, P. A.; Natan, M. J.; Freeman, R. G. *Anal. Chem.* **2002**, *74* (10), 2240–2247.
(9) Braeckmans, K.; De Smedt, S. C.; Roelant, C.; Leblans, M.; Pauwels, R.; Demeester, J. *Nat. Mater.* **2003**, *2* (3), 169–173.
(10) Dejneka, M. J.; Streltsov, A.; Pal, S.; Frutos, A. G.; Powell, C. L.; Yost, K.; Yuen, P. K.; Muller, U.; Lahiri, J. *Proc. Natl. Acad. Sci. U.S.A.* **2003**, *100* (2), 389–393.
(11) Keating, C. D.; Natan, M. J. *Adv. Mater.* **2003**, *15* (5), 451–454.
(12) Nicewarner-Pena, S. R.; Carado, A. J.; Shale, K. E.; Keating, C. D. *J. Phys. Chem. B* **2003**, *107* (30), 7360–7367.
(13) Zhi, Z. L.; Morita, Y.; Hasan, Q.; Tamiya, E. *Anal. Chem.* **2003**, *75* (16), 4125–4131.
(14) Pregibon, D. C.; Toner, M.; Doyle, P. S. *Science* **2007**, *315* (5817), 1393–1396.
(15) Qin, L.; Banholzer, M. J.; Millstone, J. E.; Mirkin, C. A. *Nano Lett.* **2007**, *7* (12), 3849–3853.
(16) Wood, D. K.; Braun, G. B.; Fraikin, J. L.; Swenson, L. J.; Reich, N. O.; Cleland, A. N. *Lab Chip* **2007**, *7* (4), 469–474.
(17) Stoermer, R. L.; Sioss, J. A.; Keating, C. D. *Chem. Mater.* **2005**, *17* (17), 4356–4361.
(18) Lee, J. H.; Wu, J. H.; Liu, H. L.; Cho, J. U.; Cho, M. K.; An, B. H.; Min, J. H.; Noh, S. J.; Kim, Y. K. *Angew. Chem., Int. Ed.* **2007**, *46* (20), 3663–3667.
(19) Piraux, L.; George, J. M.; Despres, J. F.; Leroy, C.; Ferain, E.; Legras, R.; Ounadjela, K.; Fert, A. *Appl. Phys. Lett.* **1994**, *65* (19), 2484–2486.
(20) Guo, Y. G.; Wan, L. J.; Zhu, C. F.; Yang, D. L.; Chen, D. M.; Bai, C. L. *Chem. Mater.* **2003**, *15* (3), 664–667.
(21) Liang, H. P.; Guo, Y. G.; Hu, J. S.; Zhu, C. F.; Wan, L. J.; Bai, C. L. *Inorg. Chem.* **2005**, *44* (9), 3013–3015.
(22) Choi, J. R.; Oh, S. J.; Ju, H.; Cheon, J. *Nano Lett.* **2005**, *5* (11), 2179–2183.
(23) Laocharoensuk, R.; Sattayasamitsathit, S.; Burdick, J.; Kanatharana, P.; Thavarungkul, P.; Wang, J. *ACS Nano* **2007**, *1* (5), 403–408.

10.1021/ac802670q CCC: $40.75
Published on Web 02/25/2009

nanobarcodes were tested for their potential application in miniature multiplexing bioanalysis.

EXPERIMENTAL SECTION

Fabrication of Nanobarcodes. The Co−Pt barcode nanorods were fabricated by electrochemical depositions of platinum and cobalt into the pores of anodic aluminum oxide (AAO) membranes (60 μm thick, 0.2 μm nominal pore diameter, Whatman Anodisk). Prior to the electrodeposition process, the AAO membranes were coated with a thin layer of Ag on one side to act as the working electrode. The valid area of the membrane is about 0.5 cm^2 in all experiments. Electrodeposition was carried out in a three-electrode cell with a platinum counter electrode and a saturated calomel electrode (SCE) at room temperature. The solution consisted of 30 mM chloroplatinic acid ($H_2PtCl_6 \cdot H_2O$), 500 mM cobalt sulfate ($CoSO_4 \cdot 7H_2O$), and 500 mM boric acid in deionized water. The solution pH was adjusted to 3.5 using a 5 wt % ammonia solution. Constant potentials of −1000 and −200 mV were alternatively applied to deposit cobalt segments ("spaces") and platinum segments ("bars"), respectively. The length of each segment was designed and programmatically controlled by a computer program. The electrolyte solution was removed after the electroplating, and the membrane was washed with deionized water and the back Ag films are removed by 6 M HNO_3. Finally the AAO membrane was dissolved by 2 M NaOH solution to release the nanobarcodes. The fabrication details and the resulting Co−Pt barcode nanorods were shown in Figure S1 in the Supporting Information. The EDX spectrum and XRD parents were shown in Figures S2 and S3 in the Supporting Information, respectively. Details of the fabrication process for other metallic nanobarcodes are listed in Figure S4 and the text in the Supporting Information.

Multiplexing Bioanalysis. The DNA probes and corresponding targets were purchased from SBS Genetech Co. Ltd. (Beijing, China). The probes are thiol-derivatized single strand DNA: 5′-HS-$(CH_2)_6$-GAT CAG CAG ATA GCA CCA GA-3′ (HS-Probe 1), 5′-HS-$(CH_2)_6$-GCG CAG GTT CAC TAT CTC AT-3′ (HS-Probe 2), and 5′-HS-$(CH_2)_6$-GTG GTT CAC CAG CTT TAT AG-3′ (HS-Probe 3). All HS-Probes are pretreated with 0.1 M DL-dithiothreitol (DTT) and purified with a high-performance liquid chromatography (HPLC) by the company before delivering. The targets are fluorescently labeled single-stranded DNA with complementary sequences: 5′-FAM-TC TGG TGC TAT CTG CTG ATC-3′ (abbreviated as Target 1), 5′-FAM-AT GAG ATA GTG AAC CTG CGC-3′ (Target 2), and 5′-FAM-CT ATA AAG CTG GTG AAC CAC-3′ (Target 3). The details of the multiplexing bioanalysis are described in Figure 5 and the text in the Supporting Information.

RESULTS AND DISCUSSION

The system includes a computer program, a programmable dc power supply, and an electrodeposition unit. The general process and some Morse codes used in this study are shown in Scheme 1. In this method, the coding information (letter or word) is coded as Morse codes, which can be presented as combinations of two different bar widths, namely, smaller width for "dit" and larger width for "dah". This is crucial to nanoscale encoding as this simplifies the fabrication process and minimizes the reading errors. In addition to the bar segments of different widths, spacer segments are needed to separate the bars, thus bimetallic nanobarcodes are designed in this work.

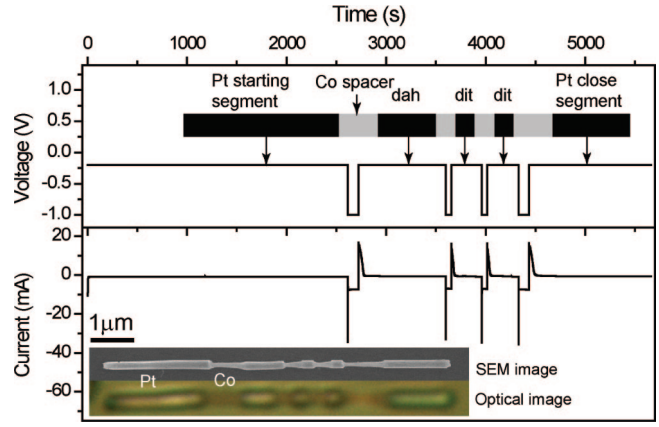

Figure 1. Programmed fabrication of Morse coded Co−Pt nanorods, which shows the schematic design of the rod (top panel), programmed time dependent voltage value and corresponding current vs time curve (middle panel), and SEM and optical images of the resulting nanorod.

Scheme 1. Scheme of the Automatically Barcode Nanorod Fabrication System, Which Can Translate Input Barcode Pattern into Corresponding Coded Nanorods[a]

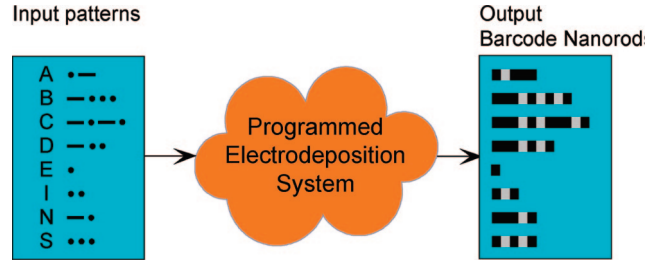

[a] The Morse code of selected characters used in this work were listed in the input patterns.

As a typical example, the Co−Pt nanobarcodes are fabricated by electrochemical depositions of platinum and cobalt into the pores of AAO membranes. Figure 1 depicts the whole programmed process to fabricate a Co−Pt nanobarcode as Morse coded letter "D". The program converts the coding information into time dependent voltage signals, as shown below in the nanobarcode design. The corresponding electrocurrent value versus time curve is also shown in the subsequent panel. Typically, it takes less than 100 min to complete one deposition process. About five batches of nanobarcodes can be produced in a working day. Thus the method is facile and fast.

Different length of Pt segments represents different information bits, i.e., short bars for "dit" and longer bars for "dah" for Morse code. Because the Morse code is not a prefix code, special features are designed to indicate the coding direction on the rods. In this work, significantly longer Pt segments are used to indicate the beginning of a code. Different lengths of Co segments are used as a spacer: short spacer segments within a Morse character and long spacer segments between different characters. In addition, at the end of each rod, a long platinum closing segment is added as a protecting segment to avoid the eroding of barcodes. The long starting and closing platinum segments also preserve

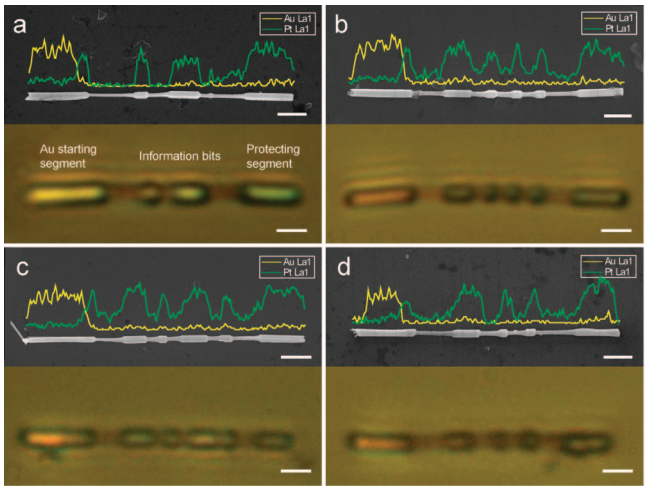

Figure 2. Different Co−Pt barcode nanorods with Au starting segments encoded by Morse "A" (a), "B" (b), "C" (c), and "D" (d). Each figure contains two panels, which are the FE-SEM image with elemental line scanning of Au and Pt compositions and the optical image of the corresponding barcode nanorods, respectively. All scale bars above are 1 μm.

the integrity of the barcode nanorods and avoid erroneous decoding.

The field emission scanning electron microscopy (FE-SEM) and optical microscopy images of the resulting nanobarcodes are shown at the bottom of Figure 1. The dah−dit−dit sequence of Morse code for letter "D" is legible in both images. More detailed characterizations of the Co−Pt nanobarcodes are shown in the Supporting Information (Figures S1−S3). Besides Co−Pt nanorods, Ni−Pt, NiCo−Pt, Au−Co−Pt, and Au−Fe nanobarcodes were fabricated with this method.

In the SEM image of the nanobarcode in Figure 1, the thinner regions are space segments consisting mainly of the element Co, while the thicker regions are bar segments consisting mainly of the element Pt. It is interesting that cobalt segments are thinner than the platinum segments. We believe that when the electrodeposition voltage was switched from −1000 (for Co deposition) to −200 mV (for Pt deposition), the Co segment formed prior to the switch was partially dissolved and became thinner. Similar results are reported by Piraus et al.[19] Such a shape difference is actually very useful information; it helps to identify Co and Pt segments, which is essential for decoding.

Similarly, nanobarcodes can be generated using various combinations of metals, such as Co, Au, Pt, and Fe. As shown in Figure 2, the nanobarcodes for letter "A", "B", "C", and "D" are produced. One particular feature of these nanobarcodes is that they have a gold segment at the beginning of each rod. We can distinguish the Au starting segments by their peculiar yellow colors in the optical image that are much different with the Pt and Co segments, and the elemental line scanning of Au and Pt compositions further validate this conclusion. These gold segments can be used as an indicator for the beginning of a code too.

One issue related to this one batch approach is that when cobalt is being deposited at low potential, platinum will also be deposited and contaminate the Co segments. To minimize the Pt contamination, in the batch solution the concentration of Co(II) is set to be more than 16 times higher than that of Pt(IV) (500 mM for Co(II) and 30 mM for Pt (IV)). Thus during Co deposition, though Pt will also be deposited, the amount of Pt in the Co segments is very low because of the low concentration of Pt(IV). This is confirmed by elemental line scanning of the nanobarcodes.

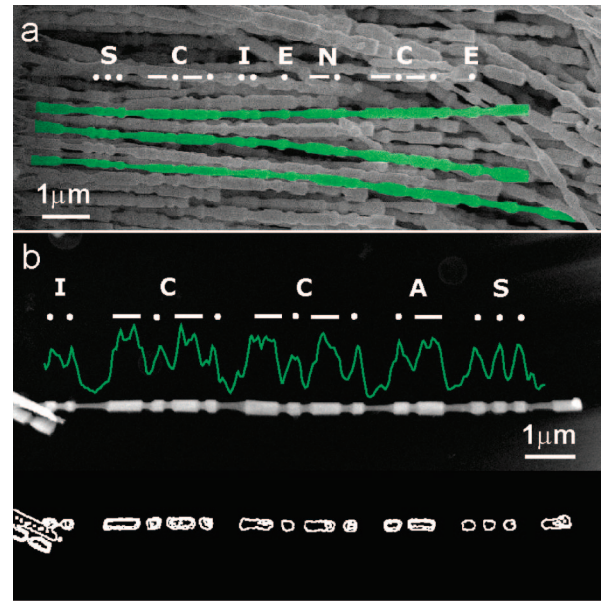

Figure 3. (a) SEM images of the nanobarcodes with Morse code "SCIENCE"; (b) nanobarcodes with "ICCAS" and two methods to decode the nanorod: readout by elemental line scanning of Pt composition (top) and the SEM images (middle) and readout result using image processing software from the SEM image (bottom).

The nanobarcodes are produced using an AAO membrane as the template, and each pore in the AAO results in one nanobarcode, and one batch can produce millions of individual barcodes (there are billions of pores in one piece of AAO membrane). Part of the ensemble of the nanobarcodes for the word "SCIENCE" is shown in Figure 3a. They can be dispersed in water and picked out as individual barcodes under a microscope.

Besides the optical microscopy, other methods can be used to decode the nanobarcodes. All "dit" and "dah" segments and the space segments are clearly recognizable in their SEM images. EDX elemental line scanning is also a reliable method to decode the nanobarcodes because all information bits are encoded as Pt segments. Figure 3b shows the SEM image and the corresponding platinum La1 EDX line scanning spectrum of a nanobarcode coded as "ICCAS", showing peaks that match well with the Pt segments in its SEM image. Furthermore, modern pattern recognition software can automatically read the barcodes from the SEM images. For example, using common image processing software, we can retrieve the barcode information from its SEM image (top panel of Figure 3b). The resulting image (bottom panel of Figure 3b) shows exactly the same pattern as the SEM image.

The number of possible code combinations in these nanobarcodes is huge. With the use of the Morse code system and current experimental setup, about 6 letters can be encoded on a 10 μm nanobarcode, thus the number of code combinations is over 300 million (26^6), far exceeding the number of carriers in any practical multiplexing arrays. Furthermore, by further extension of the length of the nanobarcodes, a nearly unlimited number of code combinations is possible.

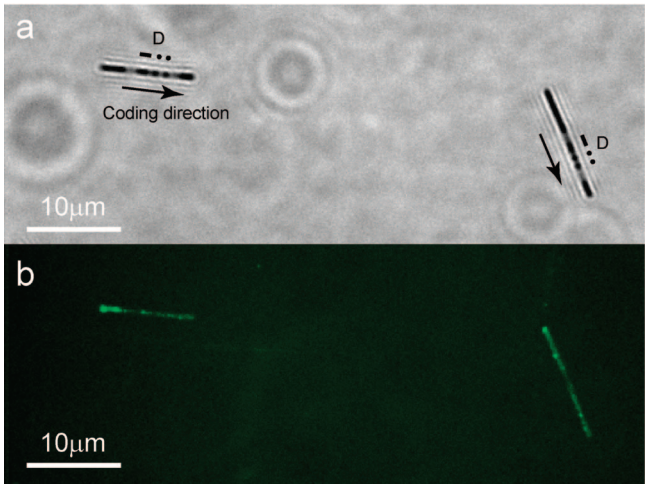

Figure 4. (a) Optical microscopy readout of barcode nanorods coded by Morse "D" loaded with thiol-derivatized oligonucleotide probes and (b) corresponding fluorescence readout of the barcodes; the barcode nanorods are fluorescent when corresponding fluorescently labeled targets exist.

Since the nanobarcodes can be identified by optical microscopy, using fluorescence imaging becomes a convenient method to identify the biomolecules interacting with the probe molecules that are immobilized on the surfaces of the nanobarcodes. There are several ways to immobilize the biological probe molecules onto the surfaces of metallic nanorods.[24−26] We chose the thiol-derivatized single strand DNA as it can attach to the metal surface via sulfur−gold linkages.[27−30] As shown in Figure 4, thiol-derivatized oligonucleotide probes are tightly attached to the Pt/Co nanobarcodes. The fluorescence image of the same two nanobarcodes shows stronger fluorescence at where Pt segments are located, indicating that the thiol-derivatized oligonucleotide probes are selectively attached to the Pt surface. Thus combining both the optical image and fluorescence image, we can build an easy to interpret multiplexing bioanalysis array.

In preliminary studies, we used three commercially available thiol-derivative single-strand DNA probe molecules for DNA sequence detection, which are labeled as HS-Probe 1, HS-Probe 2, and HS-Probe 3, respectively. The target molecules are fluorescence labeled single-strand DNA with complementary sequences to the above-mentioned probe molecules and are labeled as Target 1, Target 2, and Target 3, respectively. A three probe molecule array is built using these DNA probe molecules. The scheme of the multiplexing analysis was illustrated in Figure 5a. Three batches of nanobarcodes coded with "B", "C", and "D", respectively, were used. These nanobarcodes were loaded with different probes, respectively, and then were mixed with buffer solution to form a suspension array. After that, the array solution was added into a testing solution containing only Target 2 and Target 3 (no Target 1 was added). Parts b and c of Figure 5 show the optical image and corresponding fluorescence image of the suspension array. Nanobarcodes coded with "C" and "D" are fluorescent while "B" is not. This is exactly what is expected from experimental design. In practical bioanalysis, since the number of coded nanorods is essentially unlimited, the potential detecting ability of this strategy can be very powerful.

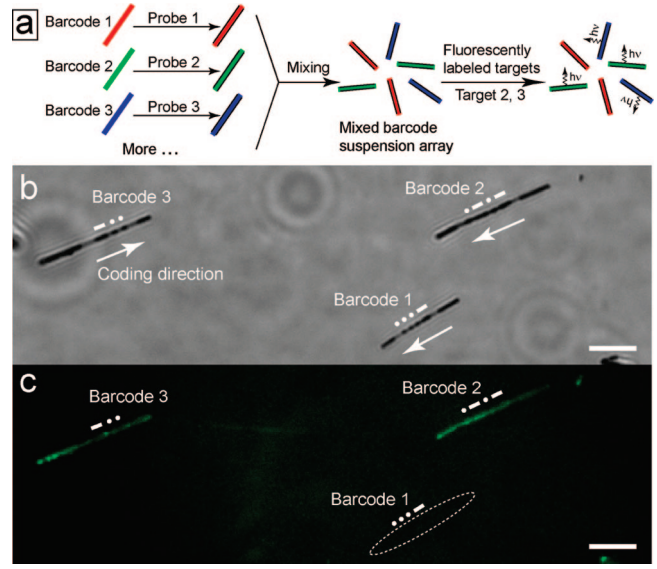

Figure 5. Multiplexing bioanalysis using nanobarcodes for fluorescence detection. (a) Scheme of the analysis array; (b) optical microscopy readout of the suspension array indicating the codes of each nanorod; and (c) corresponding fluorescence readout of the suspension array indicating that the nanorods will be fluorescent if matched target molecules exist. All scale bars are 5 μm.

CONCLUSION

We developed a programmed method to produce well-defined nanobarcodes. Each barcode can be generated directly in large quantities. The number of code combination is essentially unlimited. The barcodes are legible in optical microscopy or with other readout methods. These nanobarcodes show a promising ability in multiplexing bioanalysis.

ACKNOWLEDGMENT

We thank the financial supports from the National Natural Science Foundation of China (Grants 20673121, 20733004, and 20821003), Ministry of Science and Technology (Grants 2006CB806100, 2006CB932104, and 2009CB930400), and the Chinese Academy of Sciences.

SUPPORTING INFORMATION AVAILABLE

SEM and TEM images of other nanobarcodes and detailed experimental procedure. This material is available free of charge via the Internet at http://pubs.acs.org.

Received for review December 17, 2008. Accepted February 3, 2009.

AC802670Q

(24) Herne, T. M.; Tarlov, M. J. *J. Am. Chem. Soc.* **1997**, *119* (38), 8916–8920.
(25) Storhoff, J. J.; Elghanian, R.; Mirkin, C. A.; Letsinger, R. L. *Langmuir* **2002**, *18* (17), 6666–6670.
(26) Opdahl, A.; Petrovykh, D. Y.; Kimura-Suda, H.; Tarlov, M. J.; Whitman, L. J. *Proc. Natl. Acad. Sci. U.S.A.* **2007**, *104* (1), 9–14.
(27) Sarathy, K. V.; Kulkarni, G. U.; Rao, C. N. R. *Chem. Commun.* **1997**, (6), 537–538.
(28) Berezin, M. Y.; Wan, K. T.; Friedman, R. M.; Orth, R. G.; Raman, S. N.; Ho, S. V.; Ebner, J. R. *J. Mol. Catal. A: Chem.* **2000**, *158* (2), 567–576.
(29) Laiho, T.; Leiro, J. A.; Lukkari, J. *Appl. Surf. Sci.* **2003**, *212−213*, 525–529.
(30) Sanghamitra, N. J. M.; Mazumdar, S. *Langmuir* **2008**, *24* (7), 3439–3445.